Electronic Supplementary Material (ESI) for Physical Chemistry Chemical Physics.

Supplementary Material for the Manuscript "Quantum Confinement of Molecular Deuterium Clusters in Carbon Nanotubes: Ab-Initio Evidence for Hexagonal Close Packing"

María Pilar de Lara-Castells,[*,†] Andreas W. Hauser,[*,‡] Alexander O. Mitrushchenkov,[¶] and Ricardo Fernández-Perea[§]

†*Instituto de Física Fundamental (C.S.I.C.), Serrano 123, E-28006, Madrid, Spain*

‡*Graz University of Technology, Institute of Experimental Physics, Petersgasse 16, 8010 Graz*

¶*Université Paris-Est, Laboratoire Modélisation et Simulation Multi Echelle, MSME UMR 8208 CNRS, 5 bd Descartes, 77454 Marne-la-Vallée, France*

§*Instituto de Estructura de la Materia (C.S.I.C.), Serrano 123, E-28006, Madrid, Spain*

E-mail: Pilar.deLara.Castells@csic.es; andreas.w.hauser@gmail.com

The first section of this Supporting Information provides details of the SAPT(DFT) calculations and two tables with the parameters of our pairwise potential model. The second section presents details of the grid basis used in the adsorbate wave-functions calculations. The results with our effective potential model along the nanotube axis are presented in the third section. Finally, section 4 provides an explicit expression of the analytical spring model used to estimate the zero-point energies for the confined D_2 clusters.

S1 Details of the SAPT(DFT) Calculations

Considering a CNT$(5,5)$ tube, we have applied the SAPT(DFT) method as implemented within the `MOLPRO` electronic structure package[1] including density fitting (DF).[2] The dangling bonds were saturated with hydrogen atoms. We followed the same computational setup reported in our previous work about helium and molecular nitrogen clusters in carbon nanotubes,[3] using the Perdew-Burke-Ernzerhof (PBE) density functional,[4] and a modified version of the augmented polarized correlation-consistent triple-zeta basis[5] (aug-cc-pVTZ) for the nanotube carbon atoms as well as for the adsorbate hydrogen atoms. For the hydrogen atoms saturating the dangling bonds, the polarized correlation-consistent double-zeta basis was used instead. The modification of the carbon basis consisted in multiplying the most diffuse exponents for all angular momenta by a factor of 2.3 in order to solve linear dependence problems. The DF of Coulomb and exchange integrals employs the auxiliary basis set developed for the aug-cc-pVTZ basis by Weigend,[6] while the aug-cc-pVTZ/MP2Fit basis[7] is used for fits of integrals containing virtual orbitals. The exchange-correlation PBE potential is asymptotically corrected[8] using the ionization potential (IP) value reported in the NIST Chemistry Web Book for the H_2 molecule[9] while the IP value for the nanotube was chosen as the one estimated using the DFT PBE0 approach[10] in Ref. 3. In total, the system consists of 64 atoms, comprising an orbital basis of 2466 basis functions and an effective basis size of 4712 functions when including density fitting. The enlargement of the basis

set from cc-pVTZ to aug-cc-pVTZ on the carbon atoms rises the attractive interaction at the potential minimum by 9%; therefore, the aug-cc-pVTZ basis used in this work can be considered adequate for an accurate treatment. Considering two transverse sections of the tube, we obtained radial scans of the interaction energies plotted in Figure S1. Note that the interaction energies are very similar for the two transverse sections at the region of the potential minima, differing somewhat upon departing from the nanotube center.

S2 Pairwise Potential Model

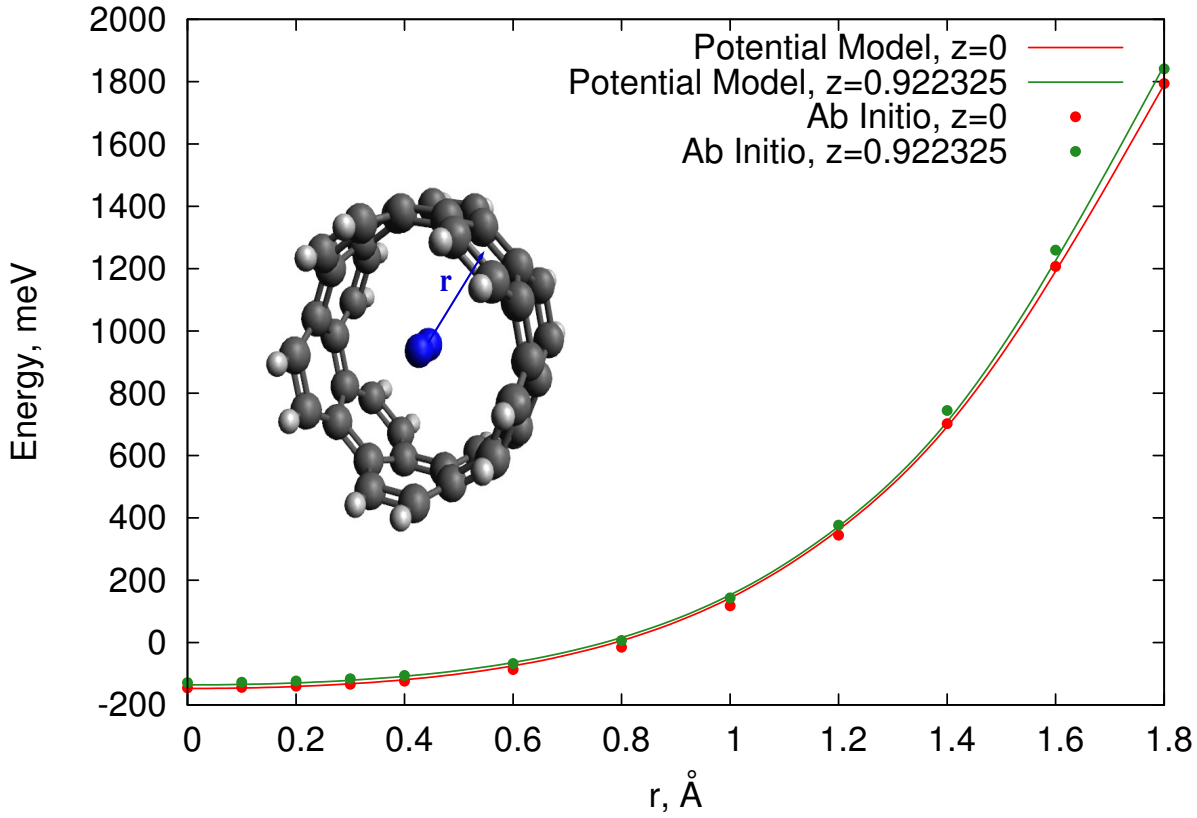

Figure S1: Radial scan of the interaction energies between a single D_2 molecule and a short carbon nanotube (sCNT) of helicity index (5,5). Our pairwise potential model is compared with reference *ab initio* calculations using the SAPT(DFT) approach considering two transverse sections of the tube located at the center ($z = 0$) and at z about 0.92 Å from the center (see the picture at the inset). The chosen tube has a length of about 3.68 Å.

The calculated *ab initio* SAPT(DFT) energies were fitted to our pairwise potential model (see main text and Ref. 3 for the details). Figure S1 shows that the potential model closely reproduces the *ab initio* energies as a function of the distance between the adsorbate and the tube center for the two considered transverse sections of the tube.

S2.1 Model parameters

Table S1 presents the values of the model parameters.

Table S1: Parameters defining the dispersionless and dispersion contributions to the D_2/CNT (or H_2/CNT) interaction energies using the additive pairwise potential model (PPM) proposed in this work. Note that the parameters for the dispersionless component are for the D_2 molecule inside the carbon nanotube.

		Dispersionless interaction energy		
R_c / Å	A / eV	α / Å^{-1}	β / Å^{-2}	γ_R
		Inside		
14.0	25.0255	1.2332	0.3843	−0.6548
		Dispersion energy		
	C_6^X / eV·Å^6	C_8^X / eV·Å^8	β^X / Å^{-1}	γ_A
X=C	12.9851	0.0	4.7307	−0.4284
X=D_2	10.7722	199.945	4.3263	–

S2.2 Parallel Configuration of Adsorbate/Nanotube Pairs: Comparison with Orientational Average

As mentioned in the main text, we have assumed that the intramolecular H_2 axis is parallel to the nanotube long axis. Using a simple model, it is possible to estimate the rotationally-averaged potential, for example for the $J = 0$ rotational state of the H_2 molecule. Indeed, assuming pairwise additivity for the H-CNT interactions, we can write

$$V_{\mathrm{H-CNT}}(r) = \frac{1}{2} V_{\mathrm{H_2-CNT}}(r)^{||}$$

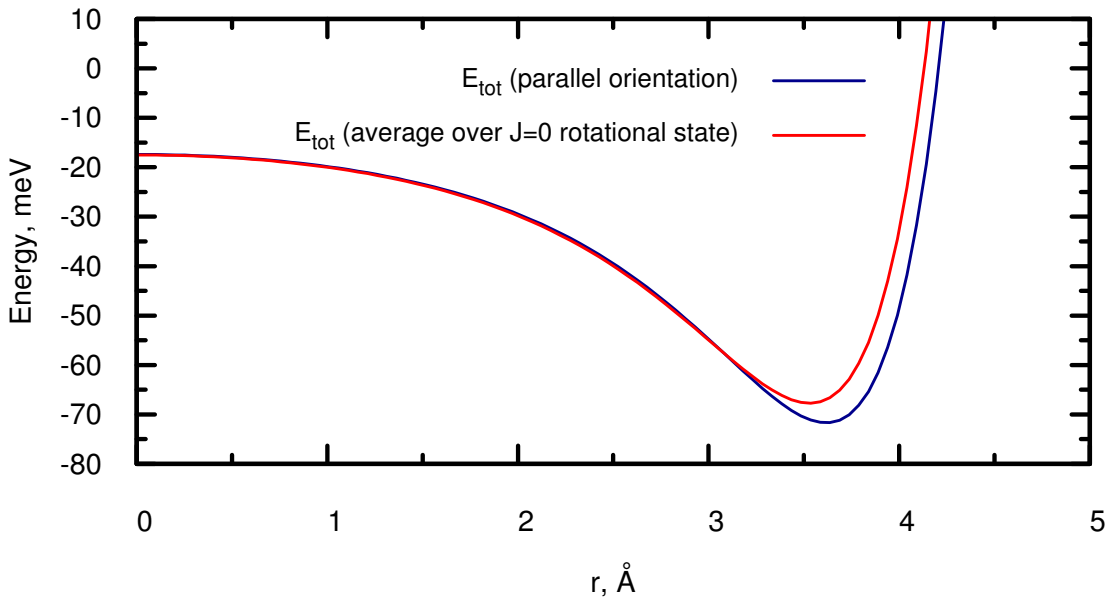

Figure S2: Comparison of the H_2/CNT(10,10) interaction potentials calculated for a parallel orientation of the H_2 molecule to the nanotube long axis and by averaging over the $J = 0$ rotational state of molecular hydrogen.

remembering that the potential $V_{\mathrm{H_2-CNT}}(r)$ goes to zero when $r \to \infty$. Then, for any orientation of the H_2 molecule, as specified by the two angles θ and ϕ, and with r now being the distance of the H_2 center-of-mass to the tube axis, the interaction potential can be written as

$$V_{\mathrm{H_2-CNT}}(r,\theta,\phi) = V_{\mathrm{H-CNT}}(r_1) + V_{\mathrm{H-CNT}}(r_2)$$

with

$$r_{1,2} = |r \pm \frac{r_0}{2}\sin\theta\cos\phi|$$

where r_0 is the equilibrium distance of the H_2 molecule. To obtain the potential corresponding to the $J = 0$ rotational state, it is sufficient to average over the two angles,

$$V_{\mathrm{H_2-CNT}}(r)^{J=0} = \frac{1}{4\pi}\int_0^{2\pi} d\phi \int_0^{\pi} \sin\theta d\theta \; V_{\mathrm{H_2-CNT}}(r,\theta,\phi).$$

Figure S2 shows the comparison between the adsorbate/CNT(10,10) interaction potential for the parallel configuration with that obtained by averaging over the $J = 0$ rotational state of molecular hydrogen. It can be seen that the differences are very small and that the parallel orientation is energetically preferred (by about 4 meV). All results of the present work are obtained using this potential.

S3 Adsorbate Wave-function Calculations: Grid Basis Sets

The adsorbate wave-function-based method has been detailed in the Supporting Information of Ref. 3. The interested reader is referred to this publication for the details. Here we simply specify the grid basis employed in our calculations, and provide explicit forms of the Hamiltonian operators for each number of adsorbate molecules.

For $N = 1$, the effective Hamiltonian is one-dimensional (1D),

$$\hat{H}^{1D} = -\frac{1}{2M}\left(\frac{\partial^2}{\partial r^2} - \frac{m^2 - 1/4}{r^2}\right) + V^{\mathrm{A-CNT}}(r).$$

where r is the cylindric coordinate associated with the distance between the adsorbate A center-of-mass and the tube center, M is the mass of the adsorbate, m is the projection of the total angular momentum on the tube long axis (fixed to zero in this work), and $V^{\mathrm{A-CNT}}$ stands for the adsorbate-nanotube interaction.

For $N = 2$, the effective Hamiltonian is four-dimensional (4D),

$$\hat{H}_\Lambda = \hat{K}_\Lambda + V^{\mathrm{A-CNT}}(r_1) + V^{\mathrm{A-CNT}}(r_2) + V_{\mathrm{A-A}}(R_{12}),$$

with Λ as the the projection of the total angular momentum on the tube long axis (fixed to zero) and $V_{\mathrm{A-A}}$ as the inter-adsorbate interaction, depending on the inter-adsorbate distance R_{12} given by

$$R_{12}^2 = r_1^2 + r_2^2 - 2r_1 r_2 \cos\phi_{12} + z_{12}^2.$$

with $\phi_{12} = \phi_2 - \phi_1$ and $z_{12} = z_2 - z_1$. The kinetic energy operator can be written as

$$\begin{aligned}\hat{K}_\Lambda \;=\; & -\frac{1}{2M}\left\{\frac{\partial^2}{\partial r_1^2} + \frac{1}{4r_1^2} + \frac{\partial^2}{\partial r_2^2} + \frac{1}{4r_2^2} + 2\frac{\partial^2}{\partial z_{12}^2}\right. \\ & \left. + \left(\frac{1}{r_1^2} + \frac{1}{r_2^2}\right)\left(\frac{\partial^2}{\partial \phi_{12}^2} - \Lambda^2\right) + \imath\Lambda\left(\frac{1}{r_2^2} - \frac{1}{r_1^2}\right)\frac{\partial}{\partial \phi_{12}}\right\}.\end{aligned}$$

For $N = 3$, the effective Hamiltonian is seven-dimensional (7D). In addition to the radial distance of the three particles (r_i, $i = 1, 2, 3$), the Hamiltonian depends on internal coordinates reading

$$
\begin{aligned}
\chi_1 &= \phi_2 - \phi_1 \\
\chi_2 &= \phi_3 - \frac{\phi_1 + \phi_2}{2} \\
t_1 &= z_2 - z_1 \\
t_2 &= z_3 - \frac{z_1 + z_2}{2}.
\end{aligned}
$$

The resulting seven-dimensional (Λ-dependent) Hamiltonian for the internal coordinates can be written as

$$\hat{H}_\Lambda = \hat{K}_\Lambda + V^{\mathrm{A-CNT}}(r_1) + V^{\mathrm{A-CNT}}(r_2) + V^{\mathrm{A-CNT}}(r_3) + V_{\mathrm{A-A}}(R_{12}) + V_{\mathrm{A-A}}(R_{13}) + V_{\mathrm{A-A}}(R_{23}),$$

and for the particular case of $\Lambda = 0$, the kinetic energy operator reads

$$
\begin{aligned}
\hat{K}_{\Lambda=0} &= -\frac{1}{2M}\left\{ \frac{\partial^2}{\partial r_1^2} + \frac{1}{4r_1^2} + \frac{\partial^2}{\partial r_2^2} + \frac{1}{4r_2^2} + \frac{\partial^2}{\partial r_3^2} + \frac{1}{4r_3^2} + 2\frac{\partial^2}{\partial t_1^2} + \frac{3}{2}\frac{\partial^2}{\partial t_2^2} \right. \\
&\left. + \left(\frac{1}{r_1^2} + \frac{1}{r_2^2}\right)\left(\frac{\partial^2}{\partial \chi_1^2} + \frac{1}{4}\frac{\partial^2}{\partial \chi_2^2}\right) + \frac{1}{r_3^2}\frac{\partial^2}{\partial \chi_2^2} + \left(\frac{1}{r_1^2} - \frac{1}{r_2^2}\right)\frac{\partial^2}{\partial \chi_1 \partial \chi_2} \right\}.
\end{aligned}
$$

To solve the corresponding $\hat{H}\Psi = \mathcal{E}\Psi$ Schrödinger equation in the real space, we used the following grid basis:

1) For the D_2/CNT and H_2/CNT systems (i.e., for the radial r coordinate), we used 1500 2D-harmonic oscillator functions with a frequency ω equal to 60 cm.$^{-1}$

2) For the $(D_2)_2$/CNT and $(H_2)_2$/CNT systems, we used the following basis:

   a) r_i $(i = 1, 2)$: 5 potential-optimized DVR functions corresponding to the radial orbitals obtained for $N = 1$.

   b) z_{12}: 1601 Sinc-DVR functions on the interval going from -80 to 80 bohr.

c) ϕ_{12}: 120 Sinc-DVR functions corresponding to $\exp(\imath m\phi_{12})$ harmonics.

3) For the $(D_2)_3$/CNT complex, the following basis was used:

a) r_i $(i = 1, 2, 3)$: 1 potential-optimized DVR functions corresponding to the radial orbitals obtained for $N = 1$.

b) t_1: 121 Sinc-DVR functions on the interval going from -30 to 30 bohr.

c) t_2: 241 Sinc-DVR functions on the interval going from -30 to 30 bohr.

d) χ_1: 90 Sinc-DVR functions corresponding to $\exp(\imath m\phi_{12})$.

e) χ_2: 120 Sinc-DVR functions corresponding to $\exp(\imath m\phi_{12})$.

Finally, within the embedding approach we used 600 2D-harmonic oscillator functions with a frequency ω equal to 1000 cm^{-1} (for r) and 121 Sinc-DVR functions on the interval going from -6 to 6 bohr.

S4 Effective Potential Model Along the Nanotube Axis

To explain how the effective inter-adsorbate interaction along the tube axis is modified by the structural arrangement of D_2 molecules, we have applied the effective potential model detailed in our previous publication.[3] Let us first consider that two D_2 molecules are encapsulated by a carbon nanotube and distributed at planes orthogonal to the tube axis, as illustrated as in the C_6 symmetry arrangements of Figure S3. The radial distributions of the two molecules are $D(r_1)$ and $D(r_2)$. We are interested in obtaining its effective inter-adsorbate interaction along the tube axis as a function of the relative distance $Z_{D_2-D_2}$ (or simply Z) . Then, the effective model interaction potential is

$$V_{\text{eff}}^{D_2-D_2}(Z) = \frac{1}{2\pi}\int dr_1 \int dr_2 \int_0^{2\pi} d\phi D(r_1)D(r_2)V_{D_2-D_2}(R), \tag{S1}$$

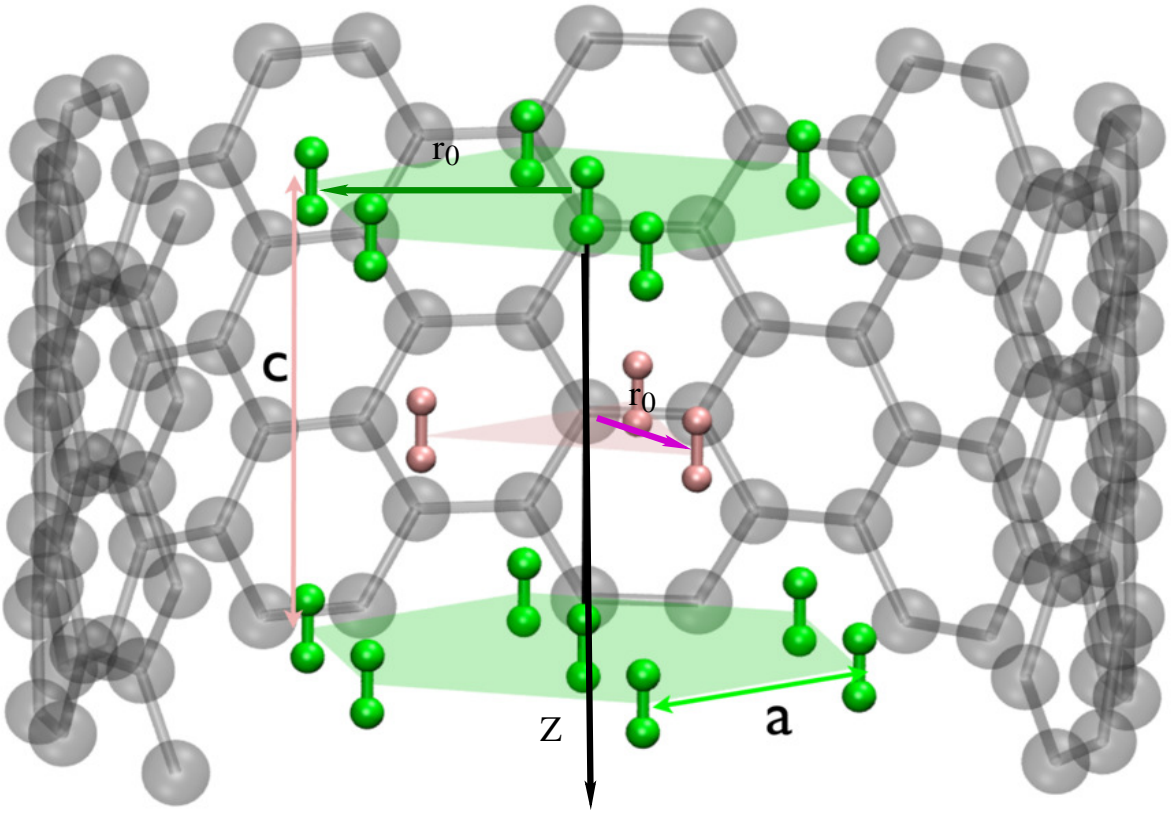

Figure S3: Figure illustrating the (10,10) nanotube with C_6 and C_3 symmetry arrangements of D_2 molecules inside. The position of the nanotube axis z is also indicated along with the average position of the D_2 molecules in the C_6 shell (referred to as r_0).

where $V_{D_2-D_2}(R)$ is the inter-adsorbate interaction potential for the isolated dimer $(D_2)_2$, and R is defined as,

$$R^2 = r_1^2 + r_2^2 - 2r_1 r_2 \cos\phi_{12} + Z^2.$$

with $\phi_{12} = \phi_2 - \phi_1$ and the densities normalized as $\int dr D(r) = 1$. We can further simplify our model by using the relation

$$D(r) = \delta(r - r_0),$$

where r_0 is the average radius defined as,

$$r_0 = \int dr\ rD(r).$$

Then, the expression of $V_{\text{eff}}^{D_2-D_2}(Z)$ in Eq. S1 is simplified to

$$V_{\text{eff}}^{D_2-D_2}(Z) = \frac{1}{2\pi}\int_0^{2\pi} d\phi_{12} V_{D_2-D_2}(R), \tag{S2}$$

where R is defined as

$$R^2 = 2r_0^2(1 - \cos\phi_{12}) + Z^2. \tag{S3}$$

From Eq. S3, it is clear that for r_0=0, $R = Z$ and the effective $D_2 - D_2$ interaction along the tube axis $V_{\text{eff}}^{D_2-D_2}(Z)$ (see Eq. S2) is the same as for the isolated dimer $V_{D_2-D_2}(R)$. This interaction potential is presented in Figure S4 (blue-colored full line) along with the supported nuclear bound state (blue-colored dashed line). Notice that the energy of the bound state (−0.86 meV) is the same as for the pure D_2 dimer (see Table 2 of the main manuscript). Upon increasing the r_0 value (see Eq. S3), the effective interaction become much less attractive (see Eq. S2) so that, for r_0=3.6 Å the resulting potential (represented with a red-colored line in Fig. S4 barely supports a bound state along the z axis. A single quasi-bound state is observed (plotted with a red-colored dashed line in Fig. S4), which is extremelly delocalized and extended towards large Z values.

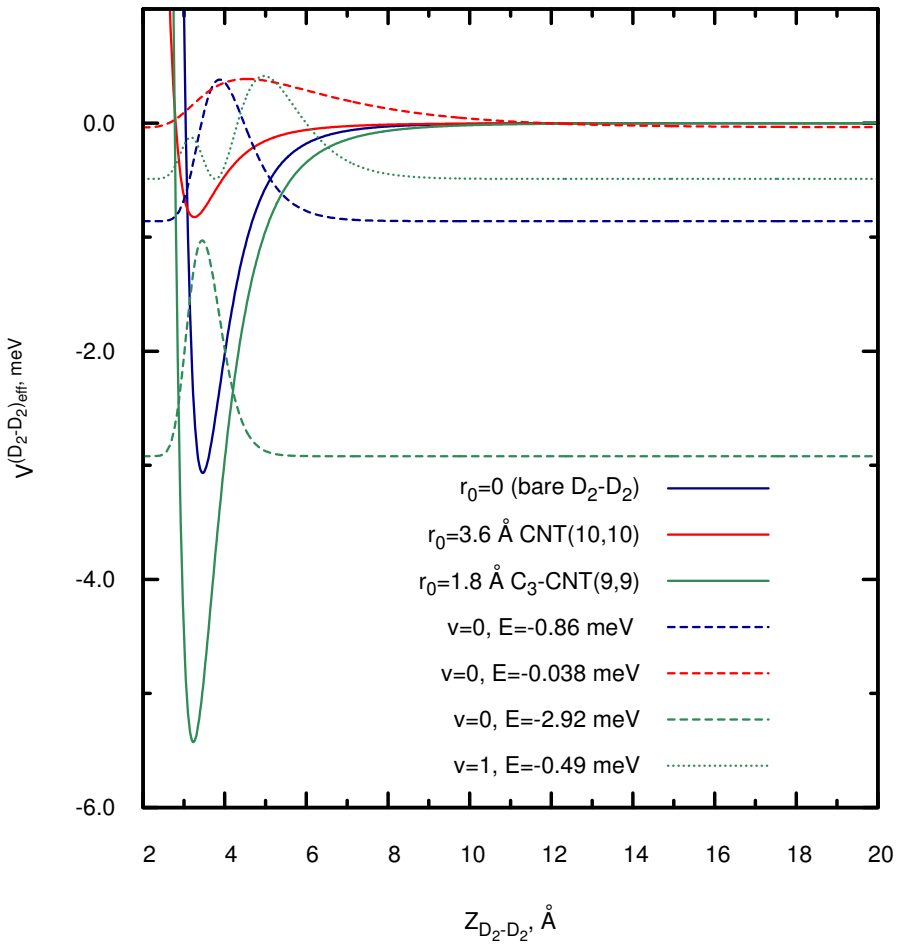

Figure S4: Effective interaction potential for two D_2 molecules as a function of the relative Z distance along the longitudinal axis of a carbon nanotube. Energies and density distributions of the supported nuclear bound states are also plotted. The potential with $r_0 = 0$ is the same as for the isolated D_2 dimer. The effective potential with $r_0 = 3.6$ Å would be defined by D_2 molecules in the (10,10) nanotube. The potential with $r_0 = 1.8$ Å corresponds to the effective interaction between a cluster of three D_2 molecules located in a C_3 symmetry structure at a plane perpendicular to the tube axis (see Figure S3), of radius equal to r_0, and a fourth D_2 molecule at a relative distance Z from the cluster.

This simplified model can also be used to estimate the interaction between a C_3 shell of three D_2 molecules, localized at an arbitrary position along z, with a single D_2 molecule, located at a distance Z from the cluster. Considering the wave-function of the cluster as a simple product of single-particle wave-functions ($N = 1$), we can apply an additive approximation and express the effective interaction as

$$V_{\text{eff}}^{\text{D}_2-3\text{D}_2(\text{C}_3)}(Z) = 3\, V_{\text{eff}}^{\text{D}_2-\text{D}_2}(Z).$$

The effective potential is represented in Figure S4 with green-colored line. Then, we simply adjust the reduced mass of the D_2-$3D_2(C_3)$ pseudo-diatomic, and get the bound states supported by the effective potential (represented with green-colored dashed lines in Figure S4). It can be observed that the potential supports two bound-states, with both the potential minimum and the energy of the ground bound-state being over twice as large as for the bare $(D_2)_2$ dimer.

S5 Analytical Spring Model Potentials

The analytical spring model potential for the *hcp*-like arrangement of 7 D_2 molecules in CNT(10,10) is of the form

$$\begin{aligned} U_{C_6} &= \frac{1}{2} f[(r_{12} - r_{\min})^2 + (r_{13} - r_{\min})^2 \\ &+ (r_{14} - r_{\min})^2 + (r_{15} - r_{\min})^2 + (r_{16} - r_{\min})^2 \\ &+ (r_{17} - r_{\min})^2 + (r_{23} - r_{\min})^2 + (r_{34} - r_{\min})^2 \\ &+ (r_{45} - r_{\min})^2 + (r_{56} - r_{\min})^2 + (r_{67} - r_{\min})^2 \\ &+ (r_{72} - r_{\min})^2], \end{aligned} \tag{S4}$$

with r_{ij} denoting the distance between atoms i and j (first atom is central). The parameters f and $r_{\min}$ are obtained by fitting this expression to PES scans over the breathing mode. Analogously, the spring model potential for the heptagonal arrangement of 8 D_2 molecules can be written as

$$\begin{aligned} U_{C_7} &= \frac{1}{2} f[(r_{12} - r_{\min})^2 + (r_{13} - r_{\min})^2 \\ &+ (r_{14} - r_{\min})^2 + (r_{15} - r_{\min})^2 + (r_{16} - r_{\min})^2 \\ &+ (r_{17} - r_{\min})^2 + (r_{18} - r_{\min})^2 + (r_{23} - r_{\min})^2 \\ &+ (r_{34} - r_{\min})^2 + (r_{45} - r_{\min})^2 + (r_{56} - r_{\min})^2 \\ &+ (r_{67} - r_{\min})^2 + (r_{78} - r_{\min})^2 + (r_{82} - r_{\min})^2], \end{aligned} \tag{S5}$$

with exactly the same nomenclature.

Figure S5 illustrates the 13 vibrational modes (plus two translations and one rotation) for the example of 8 D_2 molecules in a heptagonal, two-dimensional arrangement, confined in a carbon nanotube with helicity (10,10). The first mode in the second row corresponds to the breathing mode of the cluster. The two translations and the rotation are at the end of the last row, with their corresponding eigenvalues being close to zero.

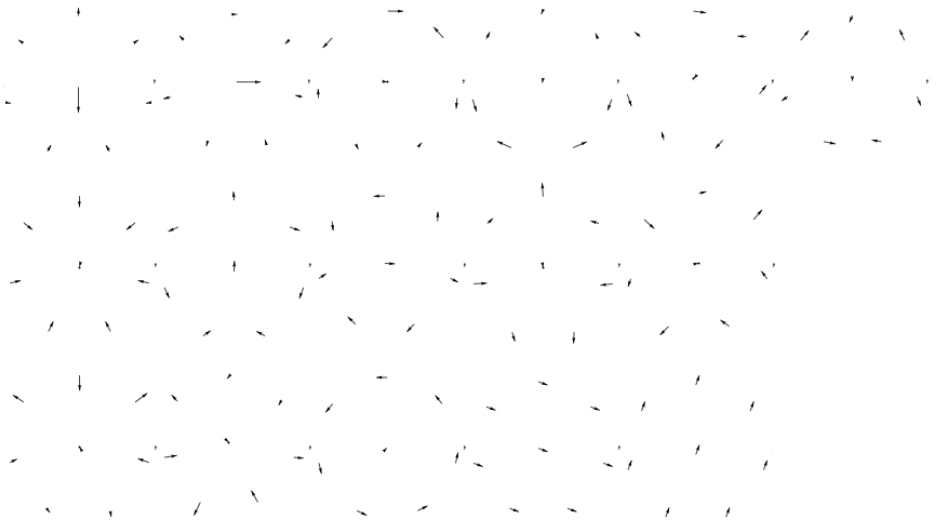

Figure S5: Vibrational modes obtained for 8 D_2 molecules in a heptagonal arrangement inside a CNT with helicity (10,10), including also the translation in x and y and the rotation around the z axis.

References

(1) Werner, H. J.; Knowles, P. J.; Knizia, G.; Manby, F. R.; Schütz, M.; Celani, P.; Korona, T.; Lindh, R.; Mitrushchenkov, A. O.; Rauhut, G. et al. MOLPRO, version 2012.1, a package of *ab initio* programs, see http://www.molpro.net.

(2) Heßelmann, A.; Jansen, G.; Schütz, M. Density-Functional-Theory Symmetry-Adapted Intermolecular Perturbation Theory with Density Fitting: A New Efficient Method to Study Intermolecular Interaction Energies. *J. Chem. Phys.* **2005**, *122*, 014103.

(3) Hauser, A. W.; Mitrushchenkov, A. O.; de Lara-Castells, M. P. Quantum Nuclear Motion of Helium and Molecular Nitrogen Clusters in Carbon Nanotubes. *J. Phys. Chem. C* **2017**, *121*, 3807–3821.

(4) Perdew, J. P.; Burke, K.; Ernzerhof, M. Generalized Gradient Approximation Made Simple. *Phys. Rev. Lett.* **1996**, *77*, 3865–3868.

(5) Woon, D. E.; Dunning, Jr., T. H. Gaussian Basis Sets for Use in Correlated Molecular Calculations. Calculation of Static Electrical Response Properties. *J. Chem. Phys.* **1994**, *100*, 2975–2988.

(6) Weigend, F. A Fully Direct RI-HF Algorithm: Implementation, Optimised Auxiliary Basis Sets, Demonstration of Accuracy and Efficiency. *Phys. Chem. Chem. Phys.* **2002**, *4*, 4285–4291.

(7) Weigend, F.; Köhn, A.; Hättig, C. Efficient Use of the Correlation Consistent Basis Sets in Resolution of the Identity MP2 Calculations. *J. Chem. Phys.* **2002**, *116*, 3175–3183.

(8) Grüning, M.; Gritsenko, O. V.; van Gisbergen, S. V. A.; Baerends, E. J. Shape Corrections to Exchange-Correlation Potentials by Gradient-Regulated Seamless Connection of Model Potentials for Inner and Outer Region. *J. Chem. Phys.* **2001**, *114*, 652–660.

(9) Lias, S. G. Ionization Energy Evaluation. NIST Chemistry Web-Book, NIST Standard Reference Database No. 69; online: http//webbook.nist.gov.

(10) Adamo, C.; Barone, V. Toward Reliable Density Functional Methods Without Adjustable Parameters: The PBE0 Model. *J. Chem. Phys.* **1999**, *110*, 6158–6170.